J Mater Sci (2008) 43:2825–2832
DOI 10.1007/s10853-008-2513-5

Simulation of aluminum foam formation and distribution uniformity

Wang Deqing · Sun Chengxin

Received: 23 October 2007 / Accepted: 29 January 2008 / Published online: 28 February 2008

Abstract Effects of bubble size formed on orifice inside an aluminum melt and bubble distribution on a foaming chamber surface were studied by experimental simulation. The bubble size formed on the liquid surface is increased with the increase in air flow rate and pressure, orifice size, and immersion depth. The orifice with 45° taper head produces smaller bubbles than that with 60° taper and flat ones. A calculation formula is established to predict bubble size formed on the orifice inside a quiescent liquid at a given surface bubble size, and the calculation agrees well with the measurement data. Orifice reciprocal agitation improves cell size uniformity of the closed-cell aluminum foam, compared with orifice rotating. Although orifice rotating is effective in producing smaller bubbles, the agitation of orifice reciprocating produces more uniform bubble distribution on the liquid surface. The bubble distribution is further improved when evenly spaced orifices are replaced by nonequidistant orifices.

Introduction

In the production of closed-cell aluminum foam, compressed air is introduced into molten aluminum composites [1, 2], and vigorous stirring of the foaming melt creates a strong vortex flow which applies shear force on the injected air. Small bubbles are formed in the melt. The bubbles rise to the melt surface, forming a liquid foam which is then mechanically conveyed off the surface of the melt and allowed to cool to form a solid slab of closed-cell aluminum foam.

As the foam cell size is critical to the performance of the aluminum foam product [2–4], the study of bubble formation in aluminum melt is important to control the property of the aluminum foam. Although numerous studies of bubble formation process were conducted [5–7], they are mainly related to the chemical processes in which the influencing factors are much less complex than the ones involved in the air-foaming aluminum melt. The variables affecting foam cell size are the type, size and volume fraction of ceramic particles, foaming temperature, melt viscosity and density, surface tensions of liquid and gas, air pressure and flow rate, agitation speed, and orifice size and number during the foam-making process.

Due to the novelty of the aluminum-melt-foaming technique, the literature on bubble formation in aluminum melt is very limited [8–11]. In the studies, the dynamic simulation of bubble formation in liquid aluminum was based on rotation stirring which produced a strong eddy around the orifices. Owing to pressure difference in different positions of the agitating vanes, various sizes of bubbles were formed on the orifices inside the liquid, and nonuniform size of bubbles on the liquid surface was obtained. Besides, the localized turbulent flow in the liquid favored directional rising of the bubbles on the orifices due to centrifugal force, resulting in localized accumulation of bubbles on liquid surface.

Since pressure on the orifice is the most pivotal factor influencing bubble size formed when other parameters are unchanged [8, 11], a constant pressure on all the orifices in liquid aluminum can bring a uniform size of bubbles in the hope of obtaining an aluminum foam with honeycomb structure.

W. Deqing (✉) · S. Chengxin
Materials Science and Engineering College, Dalian Jiaotong University, Dalian, Liaoning 116028, P.R. China
e-mail: wdq@djtu.edu.cn

This article presents an initial effort of obtaining a small and uniform size of an aluminum foam by simulations in a viscous liquid with quiescent and reciprocating orifices.

Simulation procedure

Based on the similarity principle, the simulation tank was made from acryl glass with the same dimensions ($L \times W \times H$) of $480 \times 320 \times 280$ mm^3 as the one used in practical foam production. A baffle was placed inside an acryl-glass-made rectangle tank which was divided into two portions: foaming chamber and reservoir. A polyvinyl alcohol (PVA) water solution at 20 °C was used as simulation liquid, and the viscosities of the solution were adjusted according to the viscosities of aluminum melt at foaming temperatures.

Figure 1 shows the setup for orifice-reciprocating simulation. During static simulation, compressed air was introduced into the air tube and injected into the liquid through the orifices. The orifices were 2 mm in height and had 3 mm outer diameter, and were positioned on the level part of the tube in the foaming chamber. The air flow rate and pressure were controlled by accurate variable area flow meter and reductor, respectively. During orifice-reciprocating agitation, the air tube moved horizontally with a reciprocating span of 30 mm by a crank link mechanism driven by a governor motor. The experimental setup of agitation by orifice rotation was described elsewhere [9]. The air flow rate was changed from 0.2 to 0.45 L/min, and the air pressure was 0.3–0.5 MPa. The range of the orifice diameters is 0.2–0.35 mm with the orifice external shapes of 45° and 60° taper and flat heads which are shown in Fig. 2. The variation of orifice immersion depth is 20–200 mm, and the line speeds of the agitations are 150–300 rpm.

The images of the bubbles on the liquid surface and inside the liquid were taken using a high-resolution video camera; quantitative metallography was applied to determine bubble size at different conditions, and the method of least squares was used to fit experimental simulation results of bubble size measurements.

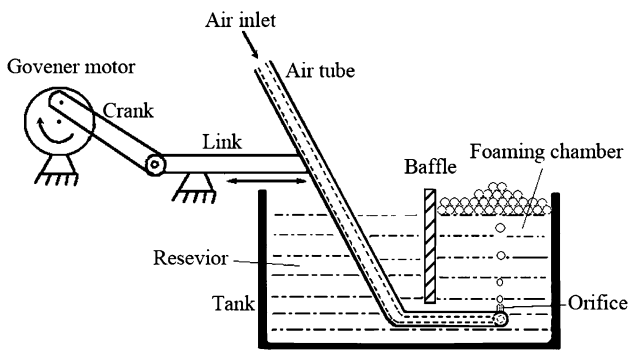

Fig. 1 Orifice-reciprocating simulation setup

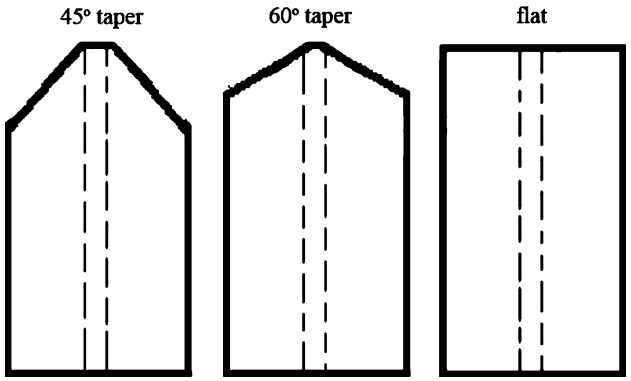

Fig. 2 External shapes of the orifices

Simulation results and discussions

Effect of influencing factors on bubble size

Air flow rate and pressure

Figure 3 shows the effect of air flow rate on bubble size in static liquid and with reciprocating agitation at 300 Hz. At the different air pressures, the bubble size is increased with the rise of air flow rate. When the air flow rate is kept constant, the bubble size is enlarged with increasing air pressure. The reason is that the inertia force of the air flowing through the small orifice becomes augmented and prolongs growth of the bubble in its formation phase with the increase in air flow rate and pressure [10]. The longer the growth time is, the more air the bubble takes in before it departs from the orifice, resulting in the formation of a larger bubble.

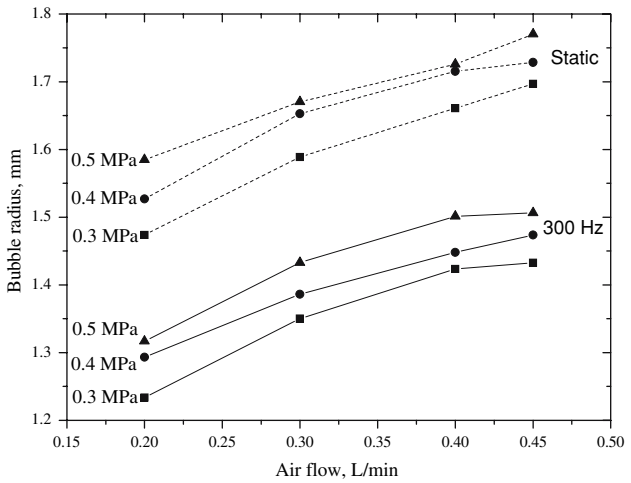

Fig. 3 Effect of air flow rate on surface bubble size with and without reciprocating agitation

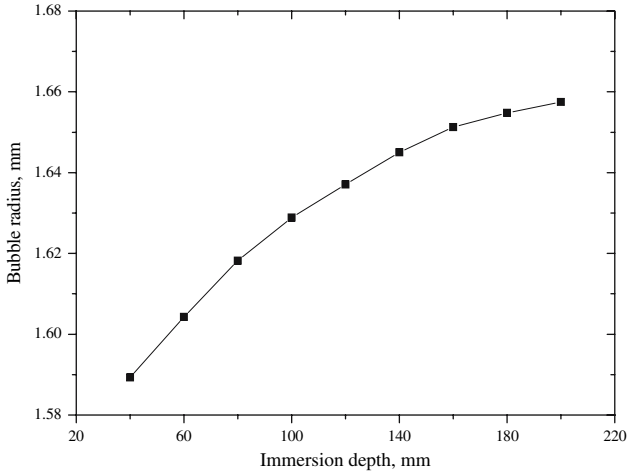

Fig. 4 Relation of bubble size and orifice immersion depth

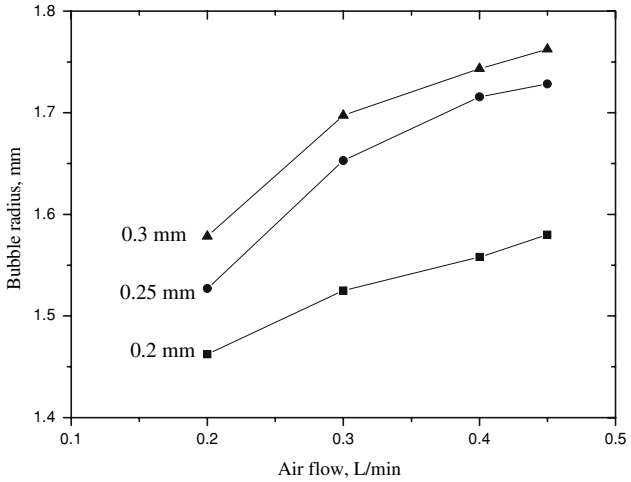

Fig. 5 Effect of air flow rate on bubble size with different orifice diameters

Compared with the static bubbling at each air flow rate and pressure in Fig. 3, the orifice agitation at 300 Hz decreases the bubble radius by nearly 20% which is about 50% volume reduction of the static ones.

Immersion depth

With the increase in the immersion depth of the orifice in the liquid, the surface bubble is increased, as shown in Fig. 4. The illustrated phenomenon comes from the pressure elevation outside the bubble with increasing the immersion depth. During bubble formation, its bottom keeps in contact with the orifice although its volume expands. In the conditions of constant air flow rate, pressure, and orifice radius, the speed of the injected air into the liquid through the orifice is unchanged. A higher static pressure of the liquid brings a lower ascending speed of the forming bubble. As the ascending speed equals the bubble radius change rate, which is an inverse ratio of its square diameter, the bubble becomes larger when its ascending speed is declined [10, 12].

Orifice size and external shape

Figure 5 shows the effect of air flow rate on bubble size with different orifice diameters. When the orifice diameter changes from 0.2 to 0.3 mm at constant air flow rate, the bubble size on the liquid surface is increased. For the bubble forming on the orifice immersed in liquid, its inner pressure has to be greater than the sum of atmospheric and static pressures plus the additive one caused by bubble curvature. The increase in orifice diameter has a twofold effect. One is to decrease bubble curvature, thereby forming a bigger bubble; another is to increase the obstructive forced on the bubble departing from orifice due to surface tension of the liquid [11–13]. This makes the bubble stay longer on the orifice, which also brings a larger bubble.

The orifice external shape also affects the bubble size on liquid surface, as shown in Fig. 6. At all air flow rates with other experimental variables constant, the size of liquid surface bubbles increased when the external shape of the orifice heads varies from 45° to 60° taper until flat. As the top area is increased in the order of 45° and 60° taper and flat head orifices, the surface tension in the interface of bubble and orifice head is raised. The greater force resulting from the surface tension favors the formation of bigger bubbles as in the case of orifice size changes.

Modeling of bubble size formed on orifice

To understand the bubble size formed at the air orifice outlet inside aluminum melt is key to manage processing

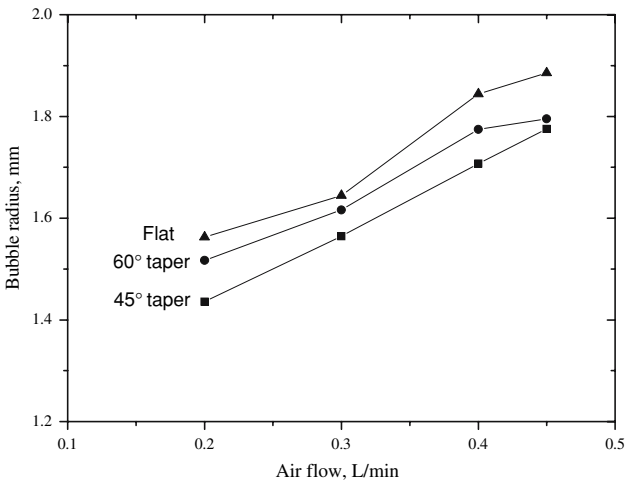

Fig. 6 Bubble size as a function of air flow rate with various shapes of orifice heads

variables and control the quality and property of aluminum foam. Owing to the opacity of aluminum melt, observation on the bubble size can only be made on surface bubbles. Thus, it is important to relate the bubble size at the air orifice inside the aluminum melt with the one on the melt surface.

Figure 7 shows the morphologies of the air bubbles formed at the top surface and the bottom of a polyvinyl alcohol solution (PVA). For simplification reasons, a sketch of the simulation is shown in Fig. 8 for a single-bubble formation process. Compressed air with a pressure of P_0 and at a rate of Q_0 flows through an orifice into the simulation solution, and a bubble forms above the air orifice at liquid depth H and flows up to the liquid surface. The radii of the orifice and the bubbles on the bottom and surface are R_0, R_1, and R_2, respectively.

Suppose the inner pressure of the bubble above the orifice is P_{b_1}, the outer pressure of the bubble P_{out} can be expressed as

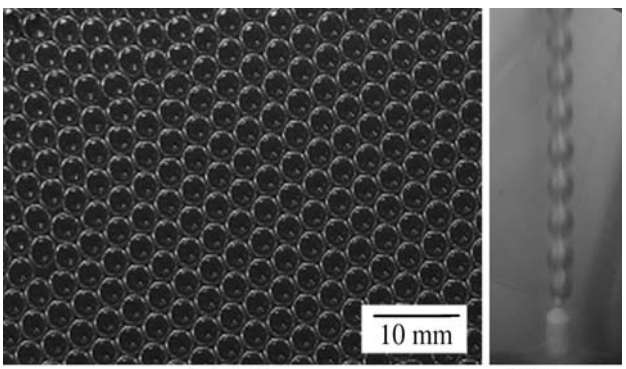

Fig. 7 Morphologies of the bubbles formed on the surface and bottom of the simulation solution

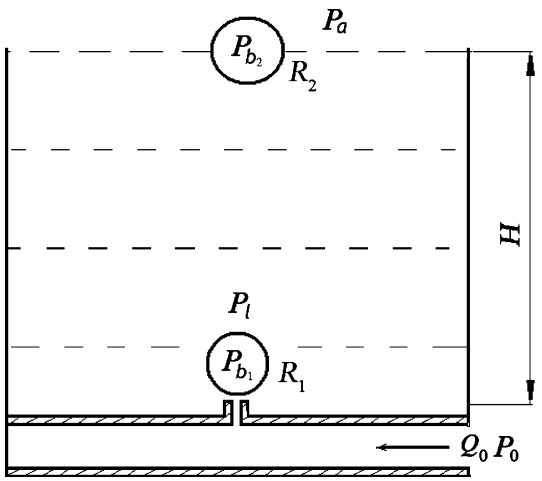

Fig. 8 Bubble formation process

$$P_{out} = P_a + P_l \tag{1}$$

where P_a is atmospheric pressure and P_l (ρgH) is hydrostatic pressure applied to the bubble. According to Yong-Laplace equation [14], the pressure difference ΔP is defined by

$$\Delta P = P_{b_1} - P_a - \rho gH = \frac{2\sigma}{R_1} \tag{2}$$

where σ is surface tension coefficient of the simulation solution.

Equation 2 indicates that the bubble radius R_1 is a constant when the pressure difference ΔP is unchanged, and the increase in the pressure difference results in a smaller bubble. Accordingly, the outer pressure of the bubble P_{out} decreases with the reduction of liquid depth during the bubble rising, resulting in the increase in bubble size. Therefore, the bubble size can be expressed as the function of the inner and outer pressure differences of the bubble, that is, $R = f(\Delta P)$.

Applying Eq. 3 to the bubbles above the orifice and on the surface in Fig. 7, the following equations are obtained

$$P_{b_1} = \frac{2\sigma}{R_1} + P_a + \rho gH \tag{3}$$

$$P_{b_2} = \frac{2\sigma}{R_2} + P_a \tag{4}$$

If the bubble shape is taken as spherical, the volumes of the bubbles at the two locations are $V_1 = \frac{4}{3}\pi R_1^3$ and $V_2 = \frac{4}{3}\pi R_2^3$, respectively. Based on perfect gas equation under constant temperature, the following relation is established

$$P_{b_1} V_1 = P_{b_2} V_2. \tag{5}$$

Equation 5 can be embodied as

$$P_{b_1} = P_{b_2}\left(\frac{R_2}{R_1}\right)^3 \tag{6}$$

Incorporating Eqs. 3, 4, and 6 achieves

$$(P_a + \rho gH)R_1^3 + 2\sigma R_1^2 - 2\sigma R_2^2 - P_a R_2^3 = 0 \tag{7}$$

and the real root solution of Eq. 7 is

$$R_1 = B^{1/3} + B^{-1/3}\left(\frac{C}{3}\right)^2 - \frac{C}{3} \tag{8}$$

where

$$B = D\left[1 + \sqrt{1 - \frac{2}{D}\left(\frac{C}{3}\right)^3}\right] - \left(\frac{C}{3}\right)^3 \left(C = \frac{2\sigma}{P_a + \rho gH}; D = \frac{\sigma R_2^2 + 0.5 P_a R_2^3}{P_a + \rho gH}\right).$$

Equation 8 is the calculation formula for the size of bubbles on the air orifice inside the liquid, given the size of

Table 1 Bubble size at different locations

Location	Depth H, mm		Bubble size R, mm								
Surface	0	Measured	1.449	1.513	1.542	1.568	1.463	1.525	1.558	1.580	1.484
Orifice	150	Calculated[a]	1.442	1.505	1.534	1.560	1.456	1.517	1.550	1.572	1.477
		Measured	1.410	1.434	1.536	1.505	1.441	1.460	1.536	1.567	1.461
		Error, %	2.2	4.7	−0.1	3.5	1.0	3.8	0.9	0.3	1.1
Surface	0	Measured	1.384	1.425	1.515	1.575	1.673	1.701	1.704	1.731	1.828
Orifice	180	Calculated[a]	1.376	1.416	1.506	1.566	1.663	1.691	1.694	1.721	1.817
		Measured	1.361	1.350	1.477	1.493	1.624	1.618	1.680	1.709	1.804
		Error, %	1.1	4.7	1.9	4.7	2.3	4.3	0.8	0.7	0.7

[a] $\sigma_{PVA} = 72$ mN/m [15]; $P_a = 1.01 \times 10^5$ Pa; $\rho_{PVA} = 1.04$ g/cm^3; $g = 9.8$ m/s^2

surface bubble whose rising speed is relatively small without causing distinct change in the outer pressure of the bubble.

Table 1 shows the results of bubble size measurement and calculation using Eq. 8. Clearly, the calculated bubble sizes are in agreement with the measured data, and the maximum error is <4.7%.

With the assumption of obtaining the same size of bubbles on Al melt and the PVA solution, Table 2 lists the comparison results according to the predictions by Eq. 8. Similarly, the calculation shows good agreement of the two bubbles at the same liquid depth with a maximum error of 0.74%.

Effect of orifice movements on surface bubble size

As indicated by hydrodynamic laws, the pressure of a liquid has an inverse relation with its flow speed; a rotating or reciprocating orifice causes the movement of its surrounding liquid, which results in a reduced pressure. Without considering the presence of transverse shear force inflicted on the bubble by the liquid movement, the pressure drop alone would produce a smaller bubble in the outlet of the orifice, compared with the one formed at the same liquid depth with a quiescent orifice. Upon the small bubble forms, its volume decreases as it rises, owing to an increasing liquid pressure. This increase is the result of gradual declining flow speed away from the orifice to static liquid. During the subsequent rising, the bubble volume increases as the static pressure decreases.

It is obvious that the agitation of the liquid around the orifice is to decrease the depth between the liquid surface and orifice where a lower pressure is obtained, resulting in the formation of a smaller air bubble. Therefore, the efficiency of liquid agitation on bubble size can be analyzed by the surface bubble size.

If an orifice moves at a constant speed v, and the bubble sizes on the liquid surface under rotation and reciprocating are R_{Rot} and R_{Rec}, respectively, the differences of the bubble sizes formed under the agitating conditions and the one in a quiescent liquid are

$$\Delta R_{Rot} = R_2 - R_{Rot} \tag{9}$$

$$\Delta R_{Rec} = R_2 - R_{Rec}. \tag{10}$$

Figure 9 shows the effect of the two movements of orifice on the reduction of bubble size, and two regression equations are also given. The correlation coefficient and standard error of the ΔR_{Rot} and ΔR_{Rec} are 0.9994337 and 0.0069861 and 0.9972787 and 0.0150804, respectively. It can be seen that the ΔR under both the orifice-rotating and orifice-reciprocating conditions shows a rapid increase with increasing agitation speed, which means a progressively decreased bubble size formed with speed rise. Furthermore, the rotation has better effect on bubble size reduction over reciprocating movement at the same orifice speed. This is due to the fact that the rotation movement produces an unvarying lower liquid pressure around the orifice spinning at a constant line speed, resulting in a consistent size of small bubbles. However, an undulate pressure field is built in the liquid along the orifice trace under reciprocating movement with a cyclic varying speed from zero to maximum. Only at maximum speed with the lowest liquid pressure can the same size of the small bubble be formed as compared with the orifice rotation.

Essentially, to obtain the small size of bubbles by liquid agitation, the pressure around the air orifice should be reduced, and the easiest way to do that is to decrease the liquid depth between the orifice and the liquid surface. In aluminum foam production by air foaming, however, the decrease in the liquid depth requires an aluminum melt with higher ceramic particle content [1], which will cause great difficulties in the preparation of the aluminum melt and the processing of the aluminum foam. Therefore, a certain depth between the orifice and liquid surface is needed for the air bubble formed on the orifice to collect ceramic particles on its surface during rise to obtain stable air bubbles on a liquid surface [17].

Table 2 Calculation of bubble size in Al melt and PVA solution

Location	Depth H, mm		Bubble size R, mm								
Surface	0		1.5	2.0	2.5	3.0	3.5	4.0	4.5	5.0	5.5
Orifice	150	PVA	1.493	1.990	2.488	2.985	3.483	3.980	4.478	4.975	5.473
		Al[a]	1.482	1.976	2.469	2.963	3.457	3.951	4.445	4.939	5.432
		Error, %	0.74	0.70	0.76	0.74	0.75	0.73	0.74	0.72	0.75
Surface	0		6.0	6.5	7.0	7.5	8.0	8.5	9.0	9.5	10.0
Orifice	150	PVA	5.970	6.468	6.965	7.463	7.960	8.458	8.955	9.453	9.950
		Al[a]	5.926	6.420	6.914	7.408	7.902	8.396	8.889	9.383	9.877
		Error, %	0.74	0.74	0.73	0.74	0.73	0.73	0.74	0.74	0.73

[a] σ_{Al} = 842 mN/m [16]; $P_a = 1.01 \times 10^5$ Pa; ρ_{Al} = 2.6 g/cm^3; g = 9.8 m/s^2

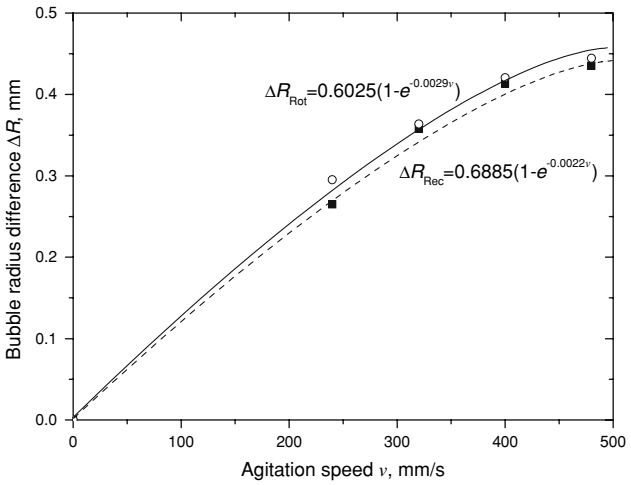

Fig. 9 Effect of orifice movements and speeds on the reduction of bubble size

Availability verification

To evaluate the applicability of Eq. 8 in practical foam production, aluminum-melt-foaming experiments were conducted at an orifice speed of 300 rpm under reciprocal movement at 660 °C. Figure 10 shows the structures of the foam produced in different conditions. Due to the difficulties in maintaining the identity of outlet diameter, air flow rate, and pressure of all the orifices, it is hard to obtain uniform bubbles on all the orifices, resulting in the obtained aluminum foam structure being far away from honeycomb. However, the uniformity of the cell size of the closed-cell aluminum foam is greatly improved, compared with the one under rotation movement of the orifices [1, 2].

The measured bubble size and the predicted one according to Eq. 8 are listed in Table 3 in which the measured data are the conversion of the foam cell size at room temperature into the bubble size at 660 °C by considering contraction of the bubbles by cooling during the foam preparation.

The difference between the measurements and predictions is because the calculation model is deduced from quiescent simulation, without considering the effects of liquid inertia force (such as the velocity of the compressed air at orifice) and shear force (such as liquid flow perpendicular to orifice axis) on the formation of bubble size under the agitation conditions [18]. As the modeling of dynamic flow field [8], however, the effects of liquid inertia and shear forces of the aluminum melt on bubble size under different agitation conditions can be summarized through experiments and associated with the orifice agitation form (ω) and speed (v). Consequently, Eq. 8 is modified by a factor $f(\omega,v)$ and changed into the following:

$$R_1 = f(\omega, v)\left[B^{1/3} + B^{-1/3}\left(\frac{C}{3}\right)^2 - \frac{C}{3}\right] \tag{11}$$

Thus, the two portions on the right side of Eq. 11 denote both dynamic and static effects on bubble size formation in the aluminum foam production, and accurate prediction of the form size can be achieved.

Distribution uniformity of surface bubbles

In view of the air-foaming aluminum melt, uniform distribution of surface bubbles is most important to produce a symmetrical foam structure with an isotropic property. Although the orifice rotation is more efficient in reducing bubble size than the orifice reciprocating does at the same line speed, the agitating vanes create a vortex around the orifice. Under the combined action of bubble buoyancy and vortex centrifugal force, the bubble formed on the orifice moves away and rises to the liquid surface along a preferred orientation, resulting in local accumulation of surface bubbles.

Figure 11 shows the bubble distribution on foaming chamber of a PVA solution when the orifice moves 3 min in 150-mm liquid depth under a constant line speed. In Fig. 11a on the upward side of the rotation center appears in a bright region where intense aggregation of bubbles occurs. Besides,

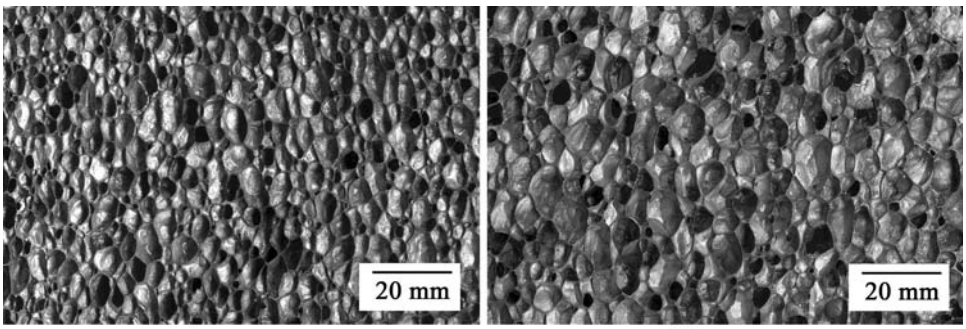

Fig. 10 Structures of different aluminum foam cell size

Table 3 Aluminum melt bubble size by measurement and prediction

Measured, mm	2.8588	3.3752	3.7508
Predicted, mm	1.2274	1.3436	1.2274
Error, %	57.1	60.2	67.3

a black flow surge region with the absence of bubbles is present at the lower left corner, resulting from a circumfluence due to the flow movement toward the side walls when the liquid disengages from the vortex core. Therefore, a single peak distribution of air volume fraction on liquid surface is predominant for the orifice rotation [11]. If aluminum foam production is conducted under this surface bubble distribution, the occurrence of severe compression and deformation of foams in the bright region and large holes in the black region is inevitable in the yielded foam material when the bubbles are conveyed off the surface vertically.

The reciprocating movement of the orifice creates laminar flow in its surrounding liquid [19], and the bubble forming on the orifice rises freely to the top surface after departing from the laminar flow field, which makes for a better distribution of surface bubbles. When orifices are spaced evenly as shown in Fig. 11b, the whole tone of the photo is relatively consistent except for a smaller flow surge region which appeared near the center orifice, indicating a greatly improved bubble distribution on the surface. When the orifices are arrayed unequally with increasing intervals toward the center orifice, the liquid surface is covered completely by bubbles as shown in Fig. 11c, and a uniform area is present on the coverage of the orifice movement. In practical production, a proper choice of the region in the top of the orifices can produce high-quality aluminum foam material with uniform density by vertical conveying of surface bubbles.

Conclusions

The bubble size formed on the liquid surface is increased with the increase in air flow rate and pressure, orifice size, and immersion depth. In the three external shapes, the orifice with 45° taper head produces the smallest bubbles compared with 60° taper and flat ones.

A calculation formula is established to predict bubble size formed on the orifice inside a quiescent liquid at the given surface bubble size, and the calculated bubble sizes agree well with the measurement data. By summarizing the effects of liquid inertia and shear forces of the aluminum

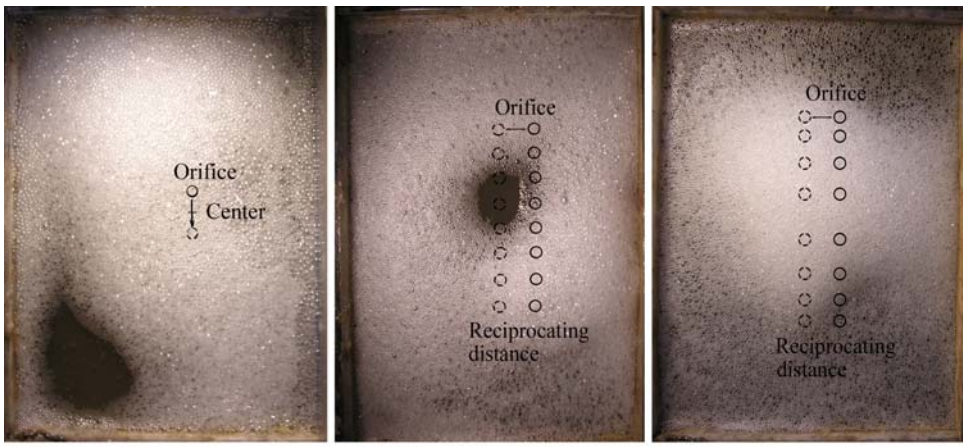

Fig. 11 Bubble distribution on foaming chamber surface under different agitations (arrows indicate orifice movement direction and solid circles stand for the original orifice position)

melt on bubble size under different agitation conditions through experiments, the static calculation model can be modified to predict aluminum foam cell size under dynamic conditions.

Under orifice reciprocal agitation, the uniformity of the cell size of the closed-cell aluminum foam is greatly improved compared with the one under orifice-rotating agitation of the aluminum melt.

Although orifice rotating is effective for producing smaller bubbles, the agitation of orifice-reciprocating movement produces more uniform distribution of the bubbles on the liquid surface of the foaming chamber. Also, the bubble distribution is further improved when evenly spaced orifices are replaced by nonequidistant orifices.

References

1. Deqing W, Ziyuan S (2003) Mater Sci Eng A 361:45
2. Deqing W, Weiwei X, Xiangjun M, Ziyuan S (2005) J Mater Sci 40:3475
3. Weigang C, Tomasz W (2001) Thin-Walled Struct 39:287
4. Firstov SA, Podrezov YN, Lugovoi NI, Slyunyaev VN, Verbilo DG (2001) Powder Metall Met Ceram 39:407
5. Nahra HK, Kamotani Y (2003) Chem Eng Sci 58:55
6. Tan RBH, Chen WB, Tan KH (2000) Chem Eng Sci 55:6259
7. Huttenhuis PJG, Kuipers JAM, van Swaaij WPM (1996) Chem Eng Sci 51:5273
8. Maozhao X, Huiling S, Hong L, Deqing W (2007) J Thermal Sci Tech 6:146
9. Deqing W, Weiwei X, Ziyuan S (2006) Mater Sci Eng A 431:298
10. Hong L, Maozhao X, Deqing W (2007) Chin J Process Eng 7:34
11. Hong L, Maozhao X, Jingdong H, Deqing W (2005) J Thermal Sci Tech 4:262
12. Yanpeng L, Bofeng B (2006) J Hydrodynamics 21:660
13. Boqin G (2000) J Nanjing Univ Chem Technol 22:1
14. Xianglin F (1989) Higher hydromechanics, 1st edn. Xian Jiaotong University Press, Xian, China, p 53 [in Chinese]
15. Changfa W, Linghua C, Kai W, Yunming L (1990) Macromol Lett 4:193
16. Hur B-Y, Park S-H, Hiroshi A (2003) Mater Sci Forum 439:51–56
17. Songlin Wang, Yi Feng, Qian Xu, Xuebin Zhang (2005) Metallic Function Mater 12:22
18. Tan RBH, Chen WB, Tan KH (2000) Chemical Eng Sci 55:6259
19. Zhenwei Y, Fulei C, Sanbao W (2006) Eng Mech 27:49